Drug Delivery and Translational Research (2022) 12:282–293
https://doi.org/10.1007/s13346-021-00937-2

ORIGINAL ARTICLE

# Ion exchange column technique as a novel method for evaluating the release of docetaxel from different lipid nanoparticles

**Mohamed Dawoud**[1,2] · **Randa Abdou**[3]

Accepted: 1 February 2021 / Published online: 25 March 2021


## Abstract

Lipid nanoparticles with their unique characters showed many advantages as carriers for anticancer drugs. To compare between these nanoparticles as carriers for anticancer drugs, it was important to evaluate and characterize their drug retention and release properties. In this study, ion exchange column is used as a new evaluation technique. Solid lipid nanoparticles (SLN), nanostructured lipid carrier (NLC), and cubic nanoparticles were prepared using the homogenization technique. Characterization of these nanoparticles was carried out by measuring particle size, zeta potential, and entrapment efficiency. The ion exchange column was used to evaluate docetaxel release from the different nanoparticles as donors to acceptor liposomes that mimic the cell membranes. Both populations were mixed and at different time points, separated using the columns. The amounts of docetaxel in the eluted nanoparticles and retained liposomes were calculated. The particle size of all donors was in the nanometer range with almost neutral zeta potential. The particle size of the acceptor liposomes was 135 nm with a high negative zeta potential −55 mV. Ion exchange columns showed excellent retention of the negative acceptor liposomes while less than 1% of the different donors were retained on the columns. Cubic nanoparticles showed the highest entrapment efficiency (95%) and the slowest drug transfer in comparison with SLN and NLC. In conclusion, the ion exchange column technique can be applied successfully to evaluate the release of docetaxel from the different lipid nanoparticles to acceptor liposomes. Cubic nanoparticles showed advantageous docetaxel incorporation and transfer over SLN and NLC.

**Keywords** Ion exchange column · Solid lipid nanoparticles · Nanostructured lipid carrier · Cubic nanoparticles · Docetaxel transfer

## Introduction

Compared with conventional cancer therapies such as surgery, radiation, and chemotherapy, many advantages have been reported for nanoparticles as drug delivery systems for anticancer drugs. These advantages could be referred for many reasons among them the improved targeting of anticancer drugs due to the small particle size of these carriers. Consequently, a reduction in anticancer drug toxicity and an increase in its concentration in cancer cells could be achieved which will lead to a lower dose and dosage regimen [1–6].

Due to the incorporation of physiological lipids and biocompatible emulsifiers in their composition, lipid nanoparticles are considered as one of the most important drug delivery systems [7, 8]. Furthermore, their small particle size and lipophilic nature will lead to a longer circulation time in the blood and accumulation of the anticancer drugs in cancer cells. Accordingly, improvement of the anticancer activity of these drugs could be obtained [9–11].

The most famous examples of these lipid nanoparticles used as carriers for anticancer drugs are liposomes, solid lipid nanoparticles ($SLN_s$), nanostructured lipid carriers (NLC), and cubic nanoparticles (cubosomes) [1, 12, 13].

$SLN_s$ were used before as carriers for many drugs due to their high safety [14, 15]. Although the $SLN_s$ were prepared using solid lipids such as trimyristin and tristearin which should give a sustained drug release, this was not achieved

✉ Mohamed Dawoud
mzdawoud@uqu.edu.sa

[1] Department of Pharmaceutics, Faculty of Pharmacy, Umm Al Qura University, Mecca, Saudi Arabia

[2] Department of Pharmaceutics and Industrial Pharmacy, Faculty of Pharmacy, Helwan-University, Cairo, Egypt

[3] Department of Pharmacognosy, Faculty of Pharmacy, Umm Al Qura University, Mecca, Saudi Arabia

in many cases as during the solidification and crystallization process of $SLN_s$, the drug might be explored to the surface which leads to a rapid drug release [16–18].

NLC is another type of lipid nanoparticle that is composed of a mixture of solid lipid and liquid oil [16, 19]. The presence of liquid oil in the composition of NLC prevents the perfect crystallization of the solid lipid. Consequently, it inhibits the drug expulsion to the outer surface as observed with $SLN_s$ [19, 20].

The newest lipid nanoparticles are the nanoparticles with a unique cubic structure which can accommodate all types of lipophilic, amphiphilic, and hydrophilic drugs [21]. These cubic nanoparticles or cubosomes are usually prepared by adding different concentrations of monoolein to water [22]. Due to their unique structure, they can incorporate a high quantity of the drug and slowly release it. Therefore, they can be considered as ideal carriers for anticancer drugs [22, 23].

In order to compare these different lipid nanoparticles as carriers for anticancer drugs, it was important to evaluate and characterize their drug retention and release properties. Many methods as dialysis-based assay, sample and separate method, and continuous-flow method have been used for measuring the drug release from such nanoparticles which encounter the same methodological problems such as blockage of the filter, binding of drugs to the filter material, and the absence of a real condition as in the bloodstream [24–29]. Furthermore, these methods usually measure the drug release in an aqueous media like a buffer solution and many drugs exhibit a poor aqueous solubility that complicates their analysis in this media [30]. Thus, other techniques were required to measure the drug release from these lipid nanoparticles to avoid such problems. Ion exchange column technique was studied as one of these techniques, and it has been previously used to measure the transfer of lipophilic molecules such as cholesterol and phosphatidylcholine between different liposomal membranes [31–33]. Such a technique worked by mixing two populations, donor and acceptor with each other and afterward separating them through ion exchange column chromatography. Therefore, one of the two populations should be charged and the other should be neutral to facilitate their separation on the columns. Consequently, ion exchange column technique does not need a filtration step and it does not suffer from the methodological problems which have been reported for the other techniques. Furthermore, the use of liposomes as acceptor particles led to a condition resembling body membranes.

In this work, docetaxel was incorporated into different lipid nanoparticles such as $SLN_s$, NLC, and cubic nanoparticles. These carriers which incorporate docetaxel were considered as the donor nanoparticle. On the other hand, acceptor liposomes were prepared by the extrusion process using S75 phospholipid. These liposomes with their phospholipid bilayers mimic the cell membranes. The entrapment efficiency of docetaxel in the different lipid nanoparticles was measured to compare between these nanoparticles. Different validation experiments were performed to determine the most suitable zeta potential for the ion exchange column technique and to ensure the efficiency of this technique for the separation of the donor lipid nanoparticles and the acceptor liposomes. Finally, a comparison of the transfer of docetaxel from the different donor lipid nanoparticles to the acceptor liposomes was carried out to find the most suitable carrier for the efficient controlled release of docetaxel.

## Materials and methods

### Materials

The triglyceride trimyristin (D114, Dynasan 114) and medium chain triglyceride Miglyol 812 were from Condea, Germany); monoolein (GMOrphic-801) was from Eastman Chemical Company (Kingsport, TN); Poloxamer 188 (F68, Lutrol F68) and poloxamer 407 (Lutrol F127) were from BASF AG (D-Ludwigshafen); 1,2-distearoyl-*sn*-glycero-3-phosphoethanolamine-*N*-[methoxy(polyethylene glycol)2000] (mPEG2000-DSPE) was purchased from Genzyme Pharmaceuticals (Cambridge, Massachusetts, USA); diethylaminoethyl (DEAE) Sepharose CL-6B Amersham Biosciences AB (S-Uppsala), lipoid S75 (Lipoid GMBH, D- Ludwigshafen), $^{3}$H-cholesteryl oleyl ether GE Healthcare (Amersham, radiochemical, Buckinghamshire, UK), and Trizma 7.4 pre-set crystals, sucrose, and sodium azide were from Sigma-Aldrich, D-Seelze; methanol and scintillation cocktail were from Carl Roth-GmbH-Karlsruhe); purified water was prepared by filtration and deionization/reverse osmosis GE Healthcare (Amersham, radiochemical, Buckinghamshire, UK).

### Preparation of the donor nanoparticles

#### Preparation of the trimyristin (D114) $SLN_s$

The hot homogenization technique was used for the preparation of trimyristin $SLN_s$. These nanoparticles were prepared as described before [34–36] by adding the aqueous phase containing the dissolved poloxamer 188 (4%) after heating to 70 °C to the molten trimyristin. This mixture was subjected to a pre-homogenization step for 1 min using Ultra-Turrax. The formed emulsion was directly transferred to a high-pressure homogenizer Microfluidizer M-110S (Microfluidics, US-Newton) and homogenized for 5 min at 500 bar and 70 °C. The

resulted nanoemulsion was loaded with docetaxel by adding 500 µl from docetaxel solution in methanol to 10 ml of the nanoemulsion followed by shaking these nanoemulsion droplets for 3 days at 25 °C in a shaking water bath. Crystallization of these nanoemulsion droplets was obtained after storage at (2–8 °C) [37].

#### Preparation of donor nanostructured lipid carriers

The nanostructured lipid carriers were prepared using 8% trimyristin as a solid lipid and 2% miglyol as a liquid lipid [38–40]. These carriers were also prepared by the hot homogenization technique where the molten trimyristin was added to miglyol oil at 70 °C. On the other hand, the aqueous phase was prepared by dissolving 4% poloxamer 188 in water followed by heating this mixture to 70 °C. The heated aqueous phase was added to the lipid mixture, and the remaining procedures were carried out as described for the preparation of $SLN_s$.

#### Preparation of the donor monoolein dispersions

To prepare monoolein dispersions with very small particle size, 5% amphiphile (monoolein + poloxamer) was used [18, 41, 42]. Briefly, monoolein was melted at 70 °C and mixed with poloxamer 407. This mixture was added dropwise to water under stirring at room temperature. The stirring of this mixture continued for 1 day to obtain the cubic gel which was transferred to a microfluidizer to be homogenized at 350 bar for 15 min at 40 °C. Finally, autoclaving of these dispersions at 121 °C for 15 min was carried out to convert vesicular structures into cubic nanoparticles [18, 41, 42]. Loading of docetaxel was carried out as described with $SLN_s$ and NLC.

#### Preparation of the acceptor unilamellar vesicles

Lipoid S75 was used to prepare these acceptor unilamellar vesicles. The lipid was dissolved in chloroform in a small bottom flask to obtain a concentration of 40 mg/ml. After drying this lipid solution, the resulted lipid film was hydrated with tris buffer saline (10 mM tris, 140 mM NaCl, pH 7.4). Finally, extrusion was carried out to this lipid suspension through 200, and 100 nm polycarbonate membranes using Liposofast extruder (Avestin Europe GmbH, D-Mannheim). Radiolabeled unilamellar vesicles were prepared using $^{3}$H-cholesteryl oleyl ether 0.1 µCi/ mg of the total vesicle lipid (2 µCi/ml) [33].

To modify the liposomes surface charge, S75 liposomes were prepared with different molar concentrations of $mPEG_{2000}$-DSPE ranging from 1 to 9%. The total lipid concentration of these surface modified liposomes was kept the same as the unmodified liposomes 40 mg/ml. These modified liposomes were loaded with docetaxel by adding 500 µl of docetaxel solution in methanol to the lipids before the drying step.

### Characterization of donors and acceptor nanoparticles

#### Particle size and zeta potential

Particle sizes of the donor $SLN_s$, NLC, cubic nanoparticles, and the acceptor unilamellar vesicles were measured by photon correlation spectroscopy (PCS) using a Zetasizer Nano ZS (Malvern Instruments Ltd., UK-Worcestershire). The measurements were performed by diluting 10 µl of the nanoparticles with 1-ml filtered demineralized water followed by measuring the particle size. The average of three measurements was calculated, and the polydispersity index (PDI) for these nanoparticles was determined. On the other hand, particle sizes of the donor cubic nanoparticles were measured before and after autoclaving with laser diffraction (LD) in combination with PIDS (polarization intensity differential scattering) using a Coulter LS 230 Particle Sizer (Beckman Coulter, D-Krefeld,). The mean particle size of these nanoparticles was calculated after 8 consecutive measurements of 90 s.

Zeta potential of the different donor nanoparticles and the acceptor unilamellar vesicles was determined with the same Malvern Zetasizer where 10 µl of the samples was diluted with 1 ml 10 mM tris buffer. The average of three measurements each consisting of 20 runs was calculated.

### Small angle X-ray diffraction measurements of the donor cubic nanoparticles

Small-angle X-ray measurements of monoolein dispersions only before and after autoclaving were performed to confirm the existence of a cubic structure in these dispersions. These measurements were performed for 1–2 h in a capillary sample holder with a SWAX camera based on a Kratky collimator system (Hecus M. Braun, Optical Systems GmbH, A-Graz) with an Iso-Debyeflex 3003 60 kV generator (Seifert-FPM D-Freiberg), an X-ray tube (copper anode) FK 61-04×12 and equipped with two position sensitive detectors (PSD-50M, M. Braun, D-Garching). The peaks spacing ratios and the lattice parameter ($a = d\sqrt{2}$) were used to determine the type of the cubic phase.

## Determination of entrapment efficiency

The percentage of docetaxel incorporated into the different donor lipid nanoparticles was calculated by using ultracentrifugation process where 1 ml of docetaxel nanoparticles was diluted with 10 ml deionized water followed by ultracentrifugation at 35,000 rpm for 15 min.

The amount of docetaxel incorporated into the cubic nanoparticles was calculated after dissolving the supernatant, which contained the creamy cubic nanoparticles, in methanol and measuring the UV absorbance at 230 nm. On the other hand, the amount incorporated into $SLN_s$ and NLC was calculated after decanting the supernatant and dissolving the precipitants, which contained SLN and NLC, in methanol and measuring the UV absorbance at 230 nm.

The percentage incorporation of docetaxel within the different lipid nanoparticles can be calculated by applying the following equation:

$$\text{EE \%} = \frac{\text{Amount of docetaxel in 1 ml nanoparticles}}{\text{Total amount of docetaxel used in the preparation of 1 ml nanoparticles}} \times 100\% \quad (1)$$

## Docetaxel transfer from the different lipid nanoparticles to the acceptor unilamellar vesicles using ion exchange column technique

### Preparation of the ion exchange column

Tris buffer saline was used to wash 50 ml of DEAE-Sepharose CL-6B. The washing process was performed twice; in every wash, 150 ml of tris buffer was used to wash the gel; and after each washing, the buffer was decanted off carefully. After the two washing processes with tris buffer, the gel was washed once again with 150-ml sucrose buffer (290 mM sucrose, 10 mM Trizma 7.4 pre-set crystals, 0.02% sodium azide, pH 7.4) followed by diluting the gel 1:1 with sucrose buffer. The length of the ion exchange columns was 5 cm with an inner diameter of 0.5 cm. At the bottom of the columns, some glass wool was placed followed by filling the columns 1 ml of the gel. For packing the columns, 2 ml of sucrose buffer was eluted, and this eluate was discarded. Before the transfer experiments were carried out, the columns were saturated with drug-free donor lipid nanoparticles in order to reduce non-specific adsorption and to improve the recovery of these nanoparticles [33]. This saturation process was performed by applying 20 µl of the donor-free nanoparticles (cubic nanoparticles, $SLN_s$, and NLC) to the columns and eluting them with 1.5-ml sucrose buffer.

### The efficient zeta potential for the ion exchange column

About 10 µl of S75 liposomes, which were prepared with different molar concentrations of $mPEG_{2000}$-DSPE and loaded with docetaxel, was placed on the columns after saturation of the columns with 20 µl of drug-free S75 liposomes. Elution was carried out with 1.5-ml sucrose buffer followed by collecting the eluate in Eppendorf tubes and diluting it with 5 ml methanol. Finally, the UV absorbance of this eluate was measured at 230 nm.

### Acceptor recovery

In Eppendorf tubes, 10 µl from the different donor lipid nanoparticles was added to 100 µl of the radiolabeled liposomes and the volume was completed to 500 µl with sucrose buffer followed by incubating these tubes in a shaking water bath at 37 °C. After 2, 8, and 24 h 200 µl from the tubes, mixtures were placed on the columns containing the gel. Elution was performed with 1.5-ml sucrose buffer, and the eluate was diluted with a 7-ml scintillation cocktail. Radioactivity of the eluate was measured, and the percentage recovery of the acceptor liposomes was calculated.

### Donor retention

About 10 µl of the different lipid nanoparticles loaded with docetaxel was placed on the columns containing the gel, which was saturated with the different lipids as mentioned before in the column preparation section. Elution was carried out with 1.5-ml sucrose buffer followed by dilution of the eluate with 5-ml methanol and measuring the UV absorbance at 230 nm.

### Docetaxel transfer to the acceptor S75 vesicles

The transfer experiments from the different lipid nanoparticles to the acceptor S75 liposomes were performed with lipid molar ratios 1:25 and 1:100 to study the effect of acceptor phospholipid concentration on drug transfer.

In Eppendorf tubes, different amounts of the donor lipid nanoparticles were mixed with different amounts of S75 liposomes and the volume was completed to 500 µl with sucrose buffer. The Eppendorf tubes were incubated at 37 °C. At different time intervals, 200 µl from the Eppendorf tubes mixture was placed on the columns followed by eluting the columns with 1.5-ml sucrose buffer. The eluate was diluted with 5-ml methanol, and the UV absorbance was

measured at 230 nm. The percentage of docetaxel retained in the different donor lipid nanoparticles was calculated by dividing the amount of docetaxel retained in the nanoparticles by the total amount of docetaxel in the donor nanoparticles at time zero. The percentage of docetaxel transferred to the acceptor S75 liposomes was determined after eluting the columns with 10-ml methanol followed by measuring UV absorbance at 230 nm. Consequently, docetaxel recovery was calculated from the percentage of drug transferred and retained.

### Transfer kinetics

Microcal Origin 6.0 software was used to analyse the transfer curves of docetaxel from the different donors to the acceptor S75 liposomes. The following equation which best fitted the transfer curves was applied for the analysis of these curves.

$$A_{acc} = A_{final} - A \times e^{-k \times t} \quad (2)$$

## Results

### Particle size and zeta potential analysis

This work utilized ion exchange column technique to measure the transfer of docetaxel from the different lipid nanoparticles to the acceptor liposomes which resemble many physiological membranes. The two populations were mixed, and at certain time points, they were separated by using these ion exchange columns.

To use this technique for the separation between the donor and acceptor, one of them should possess a charge to be held on the columns and the other should be neutral to be eluted from the columns. However, both populations should have particle sizes in the nanometer size range to avoid blocking of the columns and facilitate the elution process.

For these reasons, both particle size and zeta potential were very important features to be adjusted in order to work with the ion exchange column.

Figure 1 shows the particle size of the different lipid nanoparticles and the acceptor liposomes. S75 liposomes were prepared by extruding the lipid suspension through 200 and 100 nm polycarbonate membrane which led to liposomes with a particle size of 135 nm as seen in Fig. 1.

As illustrated in Fig. 1, the particle size of the donor $SLN_s$ and NLC was less than 150 nm with PDI less than 0.2 which indicates the homogeneity of these particles. On the other hand, the particle size of the donor cubic nanoparticles after autoclaving was 280 nm. As reported before, autoclaving was an important step to convert monoolein vesicles, which were obtained during the homogenization process, to monoolein cubic nanoparticles [41]. This transformation occurred through the aggregation of these vesicles to form the cubic structure. Thus, the particle size of the cubic nanoparticles was larger than $SLN_s$ and NLC. Additionally, the physical appearance of these monoolein dispersions confirmed the particle size results as dispersions were translucent and homogenous before autoclaving and transformed into milky

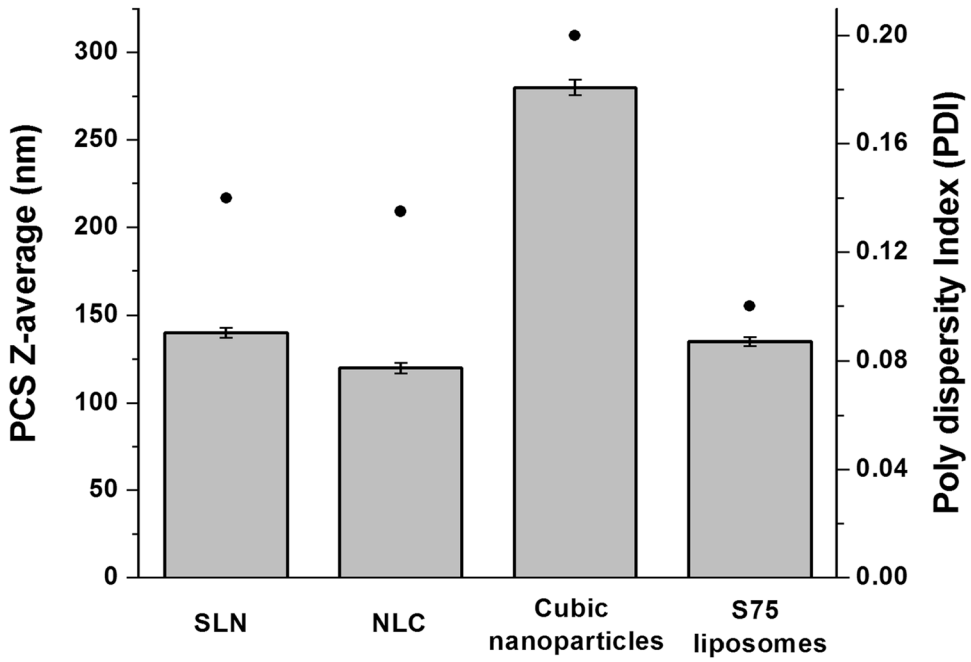


**Fig. 1** PCS z-average mean particle size (bars) and polydispersity indices (PDI, circles) of the different donor lipid nanoparticles and the acceptor S75 liposomes ($n = 3$)

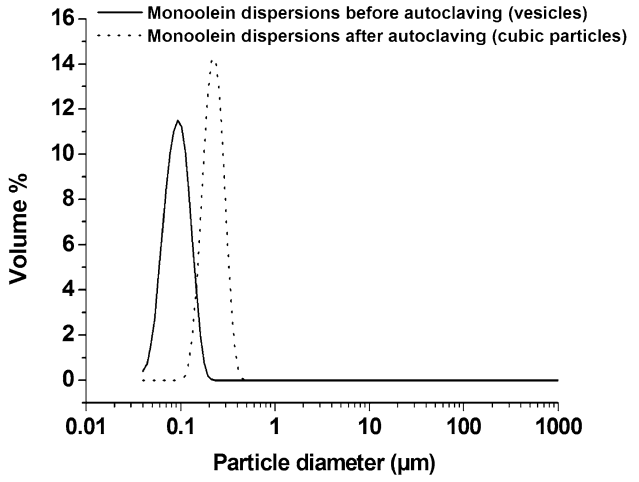


**Fig. 2** LD-PIDS particle size distributions of monoolein/poloxamer dispersions prepared with 5% amphiphile concentration (monoolein + poloxamer) before and after autoclaving

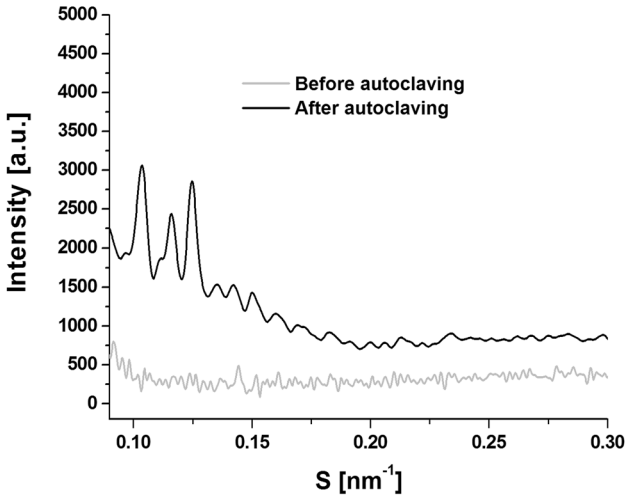


**Fig. 4** Small angle X-ray diffractograms of monoolein/poloxamer dispersions prepared with 5% amphiphile concentration (monoolein and poloxamer) before and after autoclaving, S = 1/*d* (*d* is spacing of the reflection observed)

dispersions after autoclaving. To confirm the absence of particles in the micrometer size range due to the aggregation of vesicles, particle size distribution was measured before and after autoclaving using LD-PIDS. A monomodal particle size distribution with a mean particle size of about 100 nm was observed for monoolein dispersions before autoclaving. After autoclaving, the mean particle size increased to about 300 nm due to aggregation [41] as seen in Fig. 2.

In addition to size, zeta potential is another important parameter to be considered before working with the ion exchange columns. Figure 3 illustrates the zeta potential of the donor and acceptor particles. All the different donor lipid nanoparticles possessed almost neutral zeta potential in the range between −5 and −8 mV, while the acceptor liposomes possessed a negative charge with zeta potential of about −55 mV.

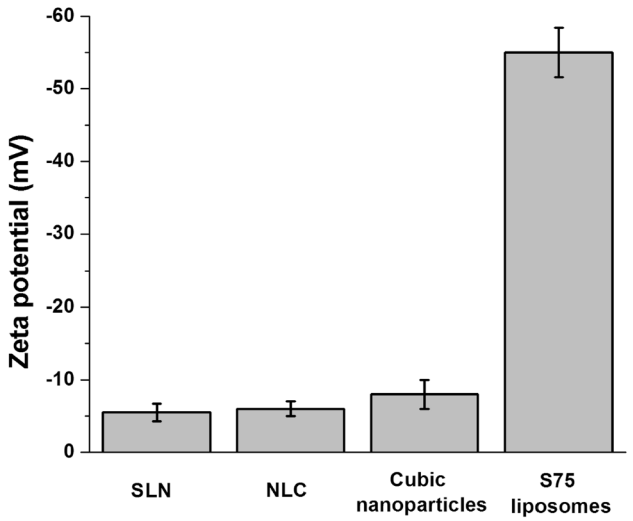


**Fig. 3** Zeta potential of the different donor lipid nanoparticles and the acceptor S75 liposomes ($n = 3$)

## Small angle X-ray diffraction measurements of the donor monoolein dispersions

It was important to carry out X-ray measurements to ensure the transformation or the aggregation of monoolein vesicles into monoolein cubic nanoparticles after the autoclaving process. As expected, no X-ray reflections were observed for the dispersions before autoclaving (Fig. 4). On the contrary, obvious reflections were observed after the autoclaving process which confirmed the existence of the cubic structure as seen in Fig. 4. The presence of three peaks with the spacing ratios of $\sqrt{2}$: $\sqrt{4}$: $\sqrt{6}$ and the lattice parameter of 14 nm confirmed the presence of the P-type cubic phase.

## Entrapment efficiency

The entrapment of docetaxel into the different donor lipid nanoparticles is illustrated in Table 1. From this table, it could

**Table 1** Entrapment efficiency of docetaxel into the different donor lipid nanoparticles

| Donor lipid nanoparticles | Entrapment efficiency (%) |
|---|---|
| SLN | 80 |
| NLC | 87 |
| Cubic nanoparticles | 95 |

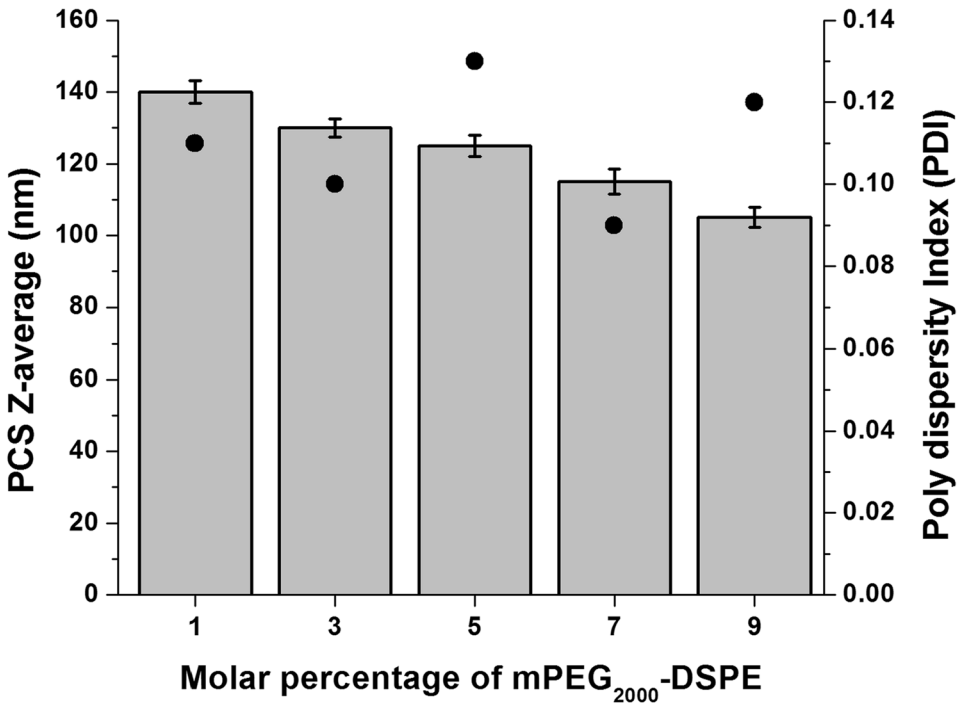


**Fig. 5** PCS z-average mean particle size (bars) and polydispersity indices (PDI, circles) of the S75 liposomes prepared with the different molar percentage of $mPEG_{2000}$-DSPE ($n = 3$)

be observed that the highest entrapment efficiency (95%) was observed for monoolein cubic nanoparticles, while the lowest entrapment efficiency (80%) was observed for SLN.

## Docetaxel transfer

### The efficient zeta potential for the ion exchange column

Figure 5 demonstrates the particle size of S75 liposomes which were prepared with different molar concentrations of mPEG-DSPE. The particle size of these liposomes ranged between 100 and 150 nm with a good PDI ranging from 0.1 to 0.14. The small particle size of these liposomes and the low PDI were very important to check the suitable zeta potential for the ion exchange column technique. Accordingly, any retention of these liposomes on the columns should be attributed to the interaction between these liposomes and the ionic gel inside the columns and not due to the blockage of the columns by large particles.

On the other hand, increasing the molar percentage of mPEG-DSPE led to a dramatic decrease in the negativity of the S75 liposomes as seen in Fig. 6. The percentage of these S75 liposomes, which had different zeta potential, eluted from the columns is demonstrated in Fig. 7. As expected, zeta potential had a great effect on the retention of these liposomes on the column where liposomes with the lowest negativity (−7 mV) showed the highest elution percent (97%). Increasing the negativity of these liposomes till −40 mV led to a decrease of the elution percent to less than 1%. Thus, the use of ion exchange columns to separate between the donor and acceptor requires that one of the two populations should be neutral or have a negative charge of not more than −10 mV to be eluted from the columns, while the other population should have a negative charge of −40 mV or more to be retained on the columns.

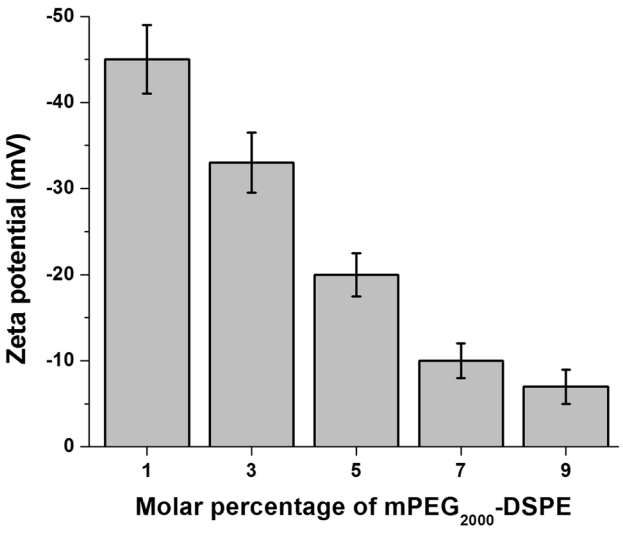


**Fig. 6** Zeta potential of the S75 liposomes prepared with the different molar percentage of $mPEG_{2000}$-DSPE ($n = 3$)

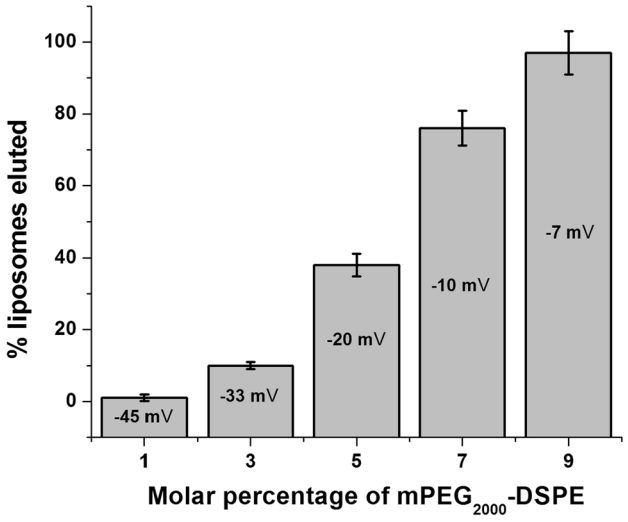


**Fig. 7** Percentage Elution of S75 liposomes prepared with the different molar percentage of $mPEG_{2000}$-DSPE and possessing different zeta potential from the ion exchange column ($n = 3$)

### Acceptor recovery

Radiolabeled S75 liposomes were used to check the retention of these acceptor particles on the ion exchange columns after mixing them with the different donor nanoparticles. As illustrated in Table 2, the maximum percent of these liposomes eluted from the columns was less than 1.5% after 24 h. This low percent of acceptor liposomes eluted from the columns indicates the good retention property of the ion exchange columns to these charged nanoparticles.

### Retention of the different donor nanoparticles

The theory behind these transfer experiments from the different donor lipid nanoparticles to the acceptor liposomes using the ion exchange column technique was the separation between both the donor and acceptor particles according to their charge. As observed in the acceptor recovery in the previous section, a very low percent of the acceptor particles was eluted from the columns. Thus, it was important to measure the elution of the different donor lipid nanoparticles. More than 99% of the different donor lipid nanoparticles were eluted from the columns as seen in Table 3.

Although the size of the donor cubic nanoparticles was large in comparison with $SLN_s$ and NLC, their elution from the column was comparable to them. The results of the acceptor recovery and donor elution indicated the suitability of the ion exchange column technique to separate between the two populations according to their charge.

**Table 2** Percentage of radiolabeled acceptor liposomes eluted from the column after incubation with the different donor lipid nanoparticles for different time intervals

| Donor lipid nanoparticles | Time (h) | Radiolabeled acceptor liposomes eluted from the column (%) |
|---|---|---|
| SLN | 2 | 0.53 ± 0.042 |
| | 8 | 0.85 ± 0.033 |
| | 24 | 1.18 ± 0.23 |
| NLC | 2 | 0.45 ± 0.021 |
| | 8 | 0.56 ± 0.032 |
| | 24 | 0.94 ± 0.094 |
| Cubic nanoparticles | 2 | 0.52 ± 0.025 |
| | 8 | 0.73 ± 0.027 |
| | 24 | 0.81 ± 0.042 |

**Table 3** Percentage of the different donor particles eluted from the column

| Donor lipid nanoparticles | Zeta potential (mV) | Donor eluted from the column (%) |
|---|---|---|
| SLN | −5 ± 1.2 | 99.5 ± 2.4 |
| NLC | −6 ± 1.1 | 99.6 ± 1.2 |
| Cubic nanoparticles | −8 ± 1.3 | 99.1 ± 2.5 |

### Docetaxel transfer from the different donor lipid nanoparticles to the acceptor S75 liposomes

The total lipid concentration of the acceptor liposomes is considered one of the most important factors affecting the transfer of docetaxel [16, 43]. To study this effect, the transfer experiments were performed with two lipid molar ratios between the donor and acceptor (1:25 and 1:100). First, the different donors showed a biphasic transfer where docetaxel transfer was slightly rapid in the first hour with both molar ratios. The highest percent of docetaxel transferred was observed with $SLN_s$ where about 35% was transferred after the first hour with molar ratio 1:100 (Fig. 8a). However, about 27% and 20% of docetaxel were transferred with the same molar ratio from NLC and cubic nanoparticles after 1 h, respectively.

After the first hour, phase two of docetaxel transfer started where the transfer was obviously slow and after 24 h about 85%, 88%, and 90% were transferred from cubic nanoparticles, $SLN_s$, and NLC, respectively.

Increasing the acceptor amount in the transfer medium led to an increase in the transfer rate and amount of docetaxel as illustrated in Fig. 8 and Table 4. Due to the initial rapid transfer from $SLN_s$ compared with NLC and cubic nanoparticles, $SLN_s$

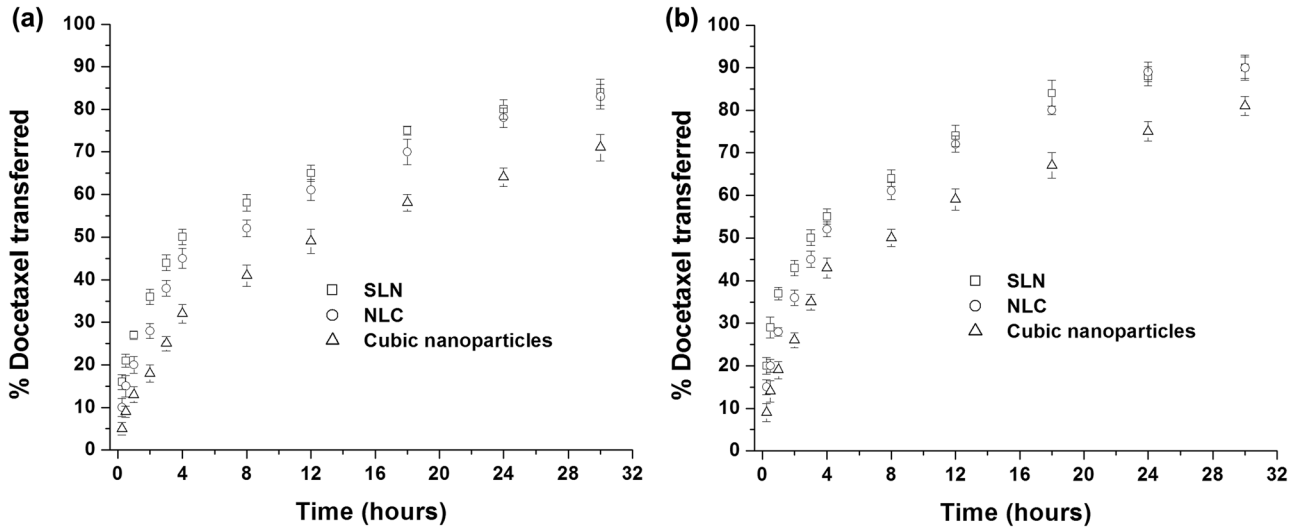


**Fig. 8** Percentage docetaxel transferred from the different donor lipid nanoparticles to the acceptor S75 liposomes with different donor: acceptor lipid molar ratios; (**a**) lipid molar ratio 1:25; (**b**) lipid molar ratio 1:100 ($n = 3$)

showed the highest transfer rate constant (0.14 and 0.17 $h^{-1}$ for the donor: acceptor 1:25 and 1:100, respectively), while cubic nanoparticles showed the lowest transfer rate constant (0.098 and 0.11 $h^{-1}$ for the donor: acceptor 1:25 and 1:100, respectively) as seen in Table 4. Finally, the recovery percent of docetaxel ranged between 95 and 103%.

## Discussion

Ion exchange column technique has been previously used to measure the transfer of lipophilic molecules such as cholesterol and phosphatidylcholine between the different liposomal membranes [31–33]. To the best of our knowledge, this is the first time this technique is used to measure the release or transfer from lipid nanoparticles other than liposomes such as cubic nanoparticles to acceptor liposomes. This ion exchange column technique was used for two purposes. The first one was to overcome the methodological problems associated with the conventional release method, while the second one was to create a model resembling the human membranes by using liposomes as acceptor particles. As mentioned before, this technique requires two important parameters to be adjusted, particle size and charge. For particle charge, one of the two populations (donor or acceptor) should be charged and the other should be neutral. Thus, poloxamer was used in the preparation of the different donor lipid nanoparticles as it stabilized the particles through a steric hindrance mechanism and not through an electrostatic repulsion mechanism. Accordingly, all the prepared donor lipid nanoparticles had an almost neutral charge. On the contrary, the acceptor liposomes were prepared with S75 which has been reported before to give liposomes with high negative surface charge as it contained fatty acids in its composition [44].

The other parameter was particle size, which should be very small in the nanometer size range, in order to facilitate the elution process and avoid the blockage of the columns by large particles. In the case of the different donor lipid nanoparticles,

**Table 4** Kinetic parameters derived from fits to the transfer curves of docetaxel from the different donors nanoparticles to the acceptor liposomes assuming transfer kinetics according to Eq. (2)

| Donor: acceptor molar ratios | Donor | Transfer rate constant K ($h^{-1}$) | Final % transferred | Equilibrium time (h) | $R^2$ for fitting |
|---|---|---|---|---|---|
| 1:25 | SLN | 0.14 ± 0.023 | 81 ± 2.9 | 27 | 0.991 |
| | NLC | 0.12 ± 0.021 | 80 ± 3.7 | 28 | 0.985 |
| | Cubic nanoparticles | 0.098 ± 0.013 | 72 ± 3.2 | 30 | 0.990 |
| 1:100 | SLN | 0.17 ± 0.031 | 87 ± 3.9 | 24 | 0.987 |
| | NLC | 0.16 ± 0.025 | 86 ± 3.7 | 24 | 0.992 |
| | Cubic nanoparticles | 0.11 ± 0.021 | 79 ± 3.7 | 26 | 0.988 |

homogenization was used to prepare particles in the nano-size range, while in the case of the acceptor liposomes, two extrusion cycles through 200 and 100 nm polycarbonate membrane were used to obtain acceptor particles in the nano-size.

The entrapment efficiency of docetaxel in the cubic nanoparticles was higher than $SLN_s$ and NLC which might be attributed to the unique structure of these cubic nanoparticles. This cubic structure was obtained from the aggregation of monoolein vesicles which means a continuous lipid bilayer was formed. This continuous lipid bilayer acted as a network or sponge that can incorporate a high percent of docetaxel. Furthermore, during crystallization of the $SLN_s$, drug expulsion could occur due to the formation of a highly ordered structure. Consequently, the lowest entrapment efficiency was observed with $SLN_s$ compared with NLC and cubic nanoparticles. In case of NLC, the incorporation of miglyol as a liquid lipid in their preparation led to the formation of crystalline particles with a less ordered inner structure which in turn decreased the escape of the drug [19, 45]. Furthermore, this liquid lipid increased the solubility of docetaxel in NLC as it is known that the drug solubility in the liquid lipids is much higher than solid lipids [46–48]. Accordingly, the entrapment efficiency of NLC was higher than $SLN_s$ but it was still lower than the unique cubic nanoparticles. Furthermore, docetaxel exhibits a poor water solubility (logP value about 2.4) that increased its entrapment into the continuous cubosomes lipid bilayers with their three-dimensional networks [49]. The lipophilic nature of docetaxel decreased its diffusion into the aqueous dispersion medium and in turn increased its entrapment within the different lipid nanoparticles.

Before performing the transfer experiments using the ion exchange column technique, validation experiments were carried out to ensure the efficacy of this technique. Initially, it was important to determine the zeta potential range of the donor and acceptor particles to be used in this technique. To determine this range and to check the effect of zeta potential on the retention and elution from the columns, S75 liposomes were prepared with different molar concentrations of $mPEG_{2000}$-DSPE. It was reported previously that the incorporation of $mPEG_{2000}$-DSPE with S75 liposomes led to a decrease in the particle size which was attributed to the arrangement of the PEG chains on the surface of the liposomes, consequently preventing the aggregation of liposomes by steric hindrance and thus decreasing their particle size [50].

Furthermore, $mPEG_{2000}$-DSPE replaced a portion of S75 lipids, and thus, the negativity of S75 liposomes decreased. Additionally, the PEG chains were arranged on the surface and shielded the negative charge of the lipid bilayer, and thus, the negativity of liposomes was reduced. A higher reduction in the negativity was obtained by increasing the percentage of $mPEG_{2000}$-DSPE. Consequently, the preparation of S75 liposomes with different molar concentrations of $mPEG_{2000}$-DSPE led to the formation of liposomes with different zeta potentials to determine the most suitable zeta potential for the particles to be either retained on the columns or eluted from them.

Accordingly, these S75 liposomes with different zeta potential were eluted from the columns. These results illustrate that for particles to be completely eluted from the columns, they should have a zeta potential of −10 mV or less negativity, while particles should have a zeta potential of higher negativity than −40 mV to be completely retained on the columns.

The acceptor liposomes had a highly negative charge (−55 mV) which should facilitate their retention, while the different donor nanoparticles exhibited an almost neutral charge that facilitated their elution from the column.

A second validation experiment was performed to ensure complete retention of the acceptor liposomes on the column after mixing them with the different donor nanoparticles. It was found that less than 2% of the charged acceptor liposomes was eluted from the columns. Despite the high negativity of these liposomes, their observed extremely low elution percent could be attributed to a small amount of fusion between the charged acceptor and the neutral donors. The third validation experiment was carried out to check the complete elution of the neutral donor nanoparticles from the column. Complete elution of all donors was obtained despite the very small difference in the particle size which indicated that there was no blockage of the columns by these donor particles. The complete elution of the donor particles could be attributed to the low negativity of these particles where their zeta potential showed negativity less than −10 mV.

The transfer of docetaxel from the different donor nanoparticles to the acceptor liposomes was a biphasic transfer where a rapid transfer was observed in the first hour followed by a slow transfer phase in the remaining time. This initial transfer phase could be referred to the location of some docetaxel molecules within the outer surface of the different nanoparticles.

The main difference in the transfer of docetaxel from the different donor lipid nanoparticles to the acceptor liposomes was observed in the initial rate and amount transferred which might be due to the differences in the amounts of docetaxel in the outer surface of the different nanoparticles. $SLN_s$ showed the highest initial transfer rate and amount which could be attributed to the location of a high amount of docetaxel at the surface of the $SLN_s$. This in turn facilitated the rapid diffusion and transfer of docetaxel to the acceptor liposomes. The location of a high amount docetaxel at the surface of the $SLN_s$ could be referred to the highly ordered crystalline structure of these particles which left a little space for the drug molecules, and consequently, drug molecules were explored to the surface of $SLN_s$.

The presence of liquid oil in the preparation of NLC led to some defects in the crystalline structure of the solid lipid which in turn decreased the escaping of docetaxel to the outer surface of NLC. On the contrary, cubic nanoparticles

illustrated the lowest rate and amount of docetaxel transfer compared with the transfer from $SLN_s$ and NLC. The main reason for these differences in the transfer rate and amount was the unique structure of these cubic nanoparticles. This unique structure was constructed through the aggregation of the monoolein vesicles after the autoclaving process. A great continuous lipid bilayer/water interfacial area was obtained which in turn incorporated docetaxel molecules within the lipid bilayer and decreased their diffusion to the acceptor liposomes [23, 51]. Finally, the percentage docetaxel recovery which ranged between 95 and 103% indicated the suitability of the ion exchange technique for evaluating the release of docetaxel from the different lipid nanoparticles.

## Conclusion

Ion exchange column technique can be applied successfully to evaluate the release of docetaxel from the different lipid nanoparticles such as cubic nanoparticles, $SLN_s$, and NLC to acceptor liposomes which mimic the physiological membrane. The ion exchange column technique showed an excellent separation between the different donor lipid nanoparticles that have been eluted from the columns and the acceptor liposomes which have been retained on the columns. Consequently, this technique can be used efficiently to measure the drug release or transfer from any donor nanoparticles to acceptor liposomes. However, both donor and acceptor should have small particle sizes and one of them should possess a charged surface while the other should be neutral. The tested cubic nanoparticles showed advantageous docetaxel incorporation and transfer over $SLN_s$ and NLC having both the highest entrapment efficiency and the lowest transfer rate. These results reveal cubic nanoparticles to be promising carriers for the anticancer drug docetaxel.

**Acknowledgements** The author would like to thank the Deanship of Scientific Research at Umm Al-Qura University for supporting this work by Grant code:19-MED-1-01-0015.

**Author contribution** Mohamed Dawoud: Conceptualization, Methodology, Writing—Original Draft, Project administration, Funding acquisition, Investigation. Randa Abdou: Methodology, Resources—Review and Editing.

**Funding** The authors received financial support from the Deanship of Scientific Research at Umm Al-Qura University by grant code 19-MED-1-01-0015.

**Data Availability** All data are included in the manuscript.

## Declarations

**Disclaimer** The authors alone are responsible for the content and writing of this article.

**Competing interests** The authors declare that they have no conflict of interest.

## References

1. Drbohlavova J, Chomoucka J, Adam V, Ryvolova M, Eckschlager T, Hubalek J, Kizek R. Nanocarriers for anticancer drugs–new trends in nanomedicine. Curr Drug Metab. 2013;14:547–64.
2. Feng L, Mumper RJ. A critical review of lipid-based nanoparticles for taxane delivery. Cancer Lett. 2013;334:157–75.
3. Yanasarn N, Sloat BR, Cui Z. Nanoparticles engineered from lecithin-in-water emulsions as a potential delivery system for docetaxel. Int J Pharm. 2009;379:174–80.
4. Yuan Q, Han J, Cong W, Ge Y, Ma D, Dai Z, Li Y, Bi X. Docetaxel-loaded solid lipid nanoparticles suppress breast cancer cells growth with reduced myelosuppression toxicity. Int J Nanomedicine. 2014;9:4829–46.
5. Chen DB, Yang TZ, Lu WL, Zhang Q. In vitro and in vivo study of two types of long-circulating solid lipid nanoparticles containing paclitaxel. Chem Pharm Bull (Tokyo). 2001;49:1444–7.
6. Wong HL, Bendayan R, Rauth AM, Li Y, Wu XY. Chemotherapy with anticancer drugs encapsulated in solid lipid nanoparticles. Adv Drug Deliv Rev. 2007;59:491–504.
7. Hwang HY, Kim IS, Kwon IC, Kim YH. Tumor targetability and antitumor effect of docetaxel-loaded hydrophobically modified glycol chitosan nanoparticles. J Control Release. 2008;128:23–31.
8. Malam Y, Loizidou M, Seifalian AM. Liposomes and nanoparticles: nanosized vehicles for drug delivery in cancer. Trends Pharmacol Sci. 2009;30:592–9.
9. Esposito E, Fantin M, Marti M, Drechsler M, Paccamiccio L, Mariani P, Sivieri E, Lain F, Menegatti E, Morari M, et al. Solid lipid nanoparticles as delivery systems for bromocriptine. Pharm Res. 2008;25:1521–30.
10. Mosallaei N, Jaafari MR, Hanafi-Bojd MY, Golmohammadzadeh S, Malaekeh-Nikouei B. Docetaxel-loaded solid lipid nanoparticles: preparation, characterization, in vitro, and in vivo evaluations. J Pharm Sci. 2013;102:1994–2004.
11. Naguib YW, Rodriguez BL, Li X, Hursting SD, Williams RO 3rd, Cui Z. Solid lipid nanoparticle formulations of docetaxel prepared with high melting point triglycerides: in vitro and in vivo evaluation. Mol Pharm. 2014;11:1239–49.
12. Alexis F, Rhee JW, Richie JP, Radovic-Moreno AF, Langer R, Farokhzad OC. New frontiers in nanotechnology for cancer treatment. Urol Oncol. 2008;26:74–85.
13. Brannon-Peppas L, Blanchette JO. Nanoparticle and targeted systems for cancer therapy. Adv Drug Deliv Rev. 2004;56:1649–59.
14. Genc L, Kutlu HM, Guney G. Vitamin B12-loaded solid lipid nanoparticles as a drug carrier in cancer therapy. Pharm Dev Technol. 2015;20:337–44.
15. Pouton CW. Lipid formulations for oral administration of drugs: non-emulsifying, self-emulsifying and 'self-microemulsifying' drug delivery systems. Eur J Pharm Sci. 2000;11:S93–8.
16. Dawoud M. Transfer of a lipophilic drug model from lipid nanoparticle carriers to a lipophilic acceptor compartment. Am J PharmTech Res. 2013;3:370–86.
17. Dawoud M. Investigations on the transfer of porphyrin from o/w emulsion droplets to liposomes with two different methods. Drug Dev Ind Pharm. 2015;41:156–62.
18. Dawoud MZ, Nasr M. Comparison of drug release from liquid crystalline monoolein dispersions and solid lipid nanoparticles using a flow cytometric technique. Acta Pharm Sin B. 2016;6:163–9.

19. Muller RH, Radtke M, Wissing SA. Nanostructured lipid matrices for improved microencapsulation of drugs. Int J Pharm. 2002;242:121–8.
20. Jores K, Haberland A, Wartewig S, Mäder K, Mehnert W. Solid lipid nanoparticles (SLN) and oil-loaded SLN studied by spectrofluorometry and raman spectroscopy. Pharm Res. 2005;22:1887–97.
21. Helledi LS, Schubert L. Release kinetics of acyclovir from a suspension of acyclovir incorporated in a cubic phase delivery system. Drug Dev Ind Pharm. 2001;27:1073–81.
22. Bei D, Zhang T, Murowchick JB, Youan BB. Formulation of dacarbazine-loaded cubosomes. Part III Physicochemical characterization AAPS PharmSciTech. 2010;11:1243–9.
23. Efrat R, Kesselman E, Aserin A, Garti N, Danino D. Solubilization of hydrophobic guest molecules in the monoolein discontinuous QL cubic mesophase and its soft nanoparticles. Langmuir. 2009;25:1316–26.
24. Boyd BJ. Characterisation of drug release from cubosomes using the pressure ultrafiltration method. Int J Pharm. 2003;260:239–47.
25. DeLuca DSS, P P. . Development of a dialysis in vitro release method for biodegradable microspheres. AAPS Pharmscitech. 2005;6:E323–8.
26. DeLuca DSS, P P. . Methods to assess in vitro drug release from injectable polymeric particulate systems. Pharm Res. 2006;23:460–74.
27. Levy MY, Benita S. Drug release from submicronized o/w emulsion - a new invitro kinetic evaluation model. Int J Pharm. 1990;66:29–37.
28. Washington C. Evaluation of non-sink dialysis methods for the measurement of drug release from colloids—effects of drug partition. Int J Pharm. 1989;56:71–4.
29. Washington C. Drug release from microdisperse systems: a critical review. Int J Pharm. 1990;58:1–12.
30. Magenheim B, Levy MY, Benita S. A new in-vitro technique for the evaluation of drug-release profile from colloidal carriers—ultrafiltration technique at low-pressure. Int J Pharm. 1993;94:115–23.
31. Van den Besselaar AM, Helmkamp GM Jr, Wirtz KW. Kinetic model of the protein-mediated phosphatidylcholine exchange between single bilayer liposomes. Biochemistry. 1975;14(9):1852–8.
32. Hellings JA, Kamp HH, Wirtz KWA, Vandeene Ll. Transfer of phosphatidylcholine between liposomes. Eur J Biochem. 1974;47:601–5.
33. McLean LR, Phillips MC. Mechanism of cholesterol and phosphatidylcholine exchange or transfer between unilamellar vesicles. Biochemistry. 1981;20:2893–900.
34. Müller RH, Mehnert W, Lucks JS, Schwarz C, zur Mühlen A, Weyhers H, Freitas C, Rühl D. Solid lipid nanoparticles (SLN)—an alternative colloidal carrier system for controlled drug delivery. Eur J Pharm Biopharm. 1995;41:62–9.
35. Venkateswarlu V, Manjunath K. Preparation, characterization and in vitro release kinetics of clozapine solid lipid nanoparticles. J Control Release. 2004;95:627–38.
36. Yang SC, Lu LF, Cai Y, Zhu JB, Liang BW, Yang CZ. Body distribution in mice of intravenously injected camptothecin solid lipid nanoparticles and targeting effect on brain. J Control Release. 1999;59:299–307.
37. Mehnert W, Mäder K. Solid lipid nanoparticles—production, characterization and applications. Adv Drug Deliv Rev. 2001;47:165–96.
38. Ling Tan JS, Roberts CJ, Billa N. Mucoadhesive chitosan-coated nanostructured lipid carriers for oral delivery of amphotericin B. Pharm Dev Technol. 2019;24:504–12.
39. Malgarim Cordenonsi L, Faccendini A, Catanzaro M, Bonferoni MC, Rossi S, Malavasi L, Platcheck Raffin R, Scherman Schapoval EE, Lanni C, Sandri G, et al. The role of chitosan as coating material for nanostructured lipid carriers for skin delivery of fucoxanthin. Int J Pharm. 2019;567:118487.
40. Rabelo RS, Oliveira IF, da Silva VM, Prata AS, Hubinger MD. Chitosan coated nanostructured lipid carriers (NLCs) for loading Vitamin D: a physical stability study. Int J Biol Macromol. 2018;119:902–12.
41. Barauskas J, Johnsson M, Johnson F, Tiberg F. Cubic phase nanoparticles (Cubosome): principles for controlling size, structure, and stability. Langmuir. 2005;21:2569–77.
42. Mohamed D, Abourehab MAS, Abdou R. Monoolein cubic nanoparticles as novel carriers for docetaxel. J Drug Deliv Sci Technol. 2020;56.
43. Dawoud M, Hashem FM. Comparative study on the suitability of two techniques for measuring the transfer of lipophilic drug models from lipid nanoparticles to lipophilic acceptors. AAPS Pharm Sci Tech. 2014;15:1551–61.
44. de Araujo SC, de Mattos AC, Teixeira HF, Coelho PM, Nelson DL, de Oliveira MC. Improvement of in vitro efficacy of a novel schistosomicidal drug by incorporation into nanoemulsions. Int J Pharm. 2007;337:307–15.
45. Yuan H, Wang LL, Du YZ, You J, Hu FQ, Zeng S. Preparation and characteristics of nanostructured lipid carriers for control-releasing progesterone by melt-emulsification. Colloids Surf B Biointerfaces. 2007;60:174–9.
46. Jores K, Mehnert W, Drechsler M, Bunjes H, Johann C, Mader K. Investigations on the structure of solid lipid nanoparticles (SLN) and oil-loaded solid lipid nanoparticles by photon correlation spectroscopy, field-flow fractionation and transmission electron microscopy. J Control Release. 2004;95:217–27.
47. Teeranachaideekul V, Boonme P, Souto EB, Muller RH, Junyaprasert VB. Influence of oil content on physicochemical properties and skin distribution of Nile red-loaded NLC. J Control Release. 2008;128:134–41.
48. Uner M. Preparation, characterization and physico-chemical properties of solid lipid nanoparticles (SLN) and nanostructured lipid carriers (NLC): their benefits as colloidal drug carrier systems. Pharmazie. 2006;61:375–86.
49. Engström S, Norden TP, Nyquist H. Cubic phases for studies of drug partition into lipid bilayers. Eur J Pharm Sci. 1999;8:243–54.
50. Garbuzenko O, Barenholz Y, Priev A. Effect of grafted PEG on liposome size and on compressibility and packing of lipid bilayer. Chem Phys Lipids. 2005;135:117–29.
51. Verma P, Ahuja M. Cubic liquid crystalline nanoparticles: optimization and evaluation for ocular delivery of tropicamide. Drug Deliv. 2016;23:3043–54.